The heat exchange Intensification in Nano-homo junction semiconductor materials

The 5th International Scientific Conference for Nanotechnology and Advanced Materials and Their Applications ICNAMA 2015 (3-4)Nov.2015

Dr. Mahmood Radhi Jubayer
College of Health & Medical Technology, Middle Technical University Baghdad
E-mail: mradhi64@yahoo.com

Abstract

In this work, it was examined mechanisms that control internal cooling device (nano-homo junction diode) depending on thermoelectric Peltier effect, resulting in structures that are optimized thermal management. Peltier coefficient for short-length diode is theoretically investigated. It is found that the cooling power is governed by the carrier concentration, current density and the ratio of n-type region width to p-type region width. It has been determined the optimum value of the cooling power at the junction of ZnO in the optimum density at doping symmetrically on a certain value. The cooling power, temperature difference (temperature between the contact and the junction) and dimensionless figure of merit are found in this material for different thicknesses, then comparing between them. It has been simulated the homo junction diode using a MATLAB software with numerically calculated the Peltier coefficient for each layer in these diodes. It has been found that nano-homojunction introduce a significant improvement in the internal cooling performance.

Keywords: ZnO, Peltier effect, heat exchange**,** thermoelectric cooler, homojunction, quantum well

تكثيف التبادل الحراري في مواد أشباه الموصلات ذات الوصلة المتجانسة النانوية

الخلاصة:

في هذا العمل، تم اختبار الآليات التي تتحكم في نبيطة التبريد الداخلي (الصمام الثنائي المتجانس الوصلة النانوي) اعتمادا على تأثير بلتيير، التي تؤدى إلى التراكيب الأمثل للتحكم الحراري. حققنا معامل بلتيير للطول القصير للصمام الثنائي نظريا. تبين أن قوة التبريد تحكمها تركيز الناقل، وكثافة التيار والنسبة بين عرض المنطقة ذات النوع n الى عرض المنطقة ذات نوع p. تم تحديد القيمة المثلى لقوة التبريد عند الوصلة لمادة أكسيد الزنك في الكثافة المثلى عند التطعيم المتناظر عند قيمة معينة. تم التحقق من قدرة التبريد والفرق في درجة حرارة التبريد (درجة الحرارة بين نقطة الاتصال والوصلة) ومعامل الاستحقاق في هذه المادة لاسماك مختلفة ومن ثم المقارنة بينهما. تم محاكاة الصمام الثنائي المتجانس الوصلة النانوي باستخدام برنامج ماتلاب مع احتساب معامل بلتيير عدديا لكل طبقة في هذا الثنائي. وقد وجد أن المتجانس الوصلة النانوي يدخل تحسنا كبيرا في أداء التبريد الداخلي

الكلمات المرشدة: اكسيد الزنك, تأثير بلتير, تبادل حراري, مبرد كهروحراري, ثنائي متجانس الوصلة, بئر كمي

INTRODUCTION

One of the most significant problems that affect the performance and operating lifetime of semiconductor devices is the height of degree excessive heat. Excessive heat can cause rapid or gradual change occurs to the device characteristics [1, 2]. Therefore, in many applications especially nano-electronics and optoelectronics, the issue of the control and the stabilization of temperature makes it source of the prime interest for improves the performance of devices. Thermal

https://doi.org/10.30684/etj.33.5B.7
2412-0758/University of Technology-Iraq, Baghdad, Iraq
This is an open access article under the CC BY 4.0 license http://creativecommons.org/licenses/by/4.0

management and access to temperature stabilization is accomplished using thermoelectric (TE) coolers [3, 4]. The basic concept behind of all thermoelectric cooling devices is called the Peltier effect. TE cooling effect of a material can be gauged by the Peltier coefficient Π, that relates the heat carried (*Q*) by the charges to the electrical current through $Q = \Pi \times I$ [5, 6]. Physical origin of the traditional Peltier cooler is based on Bulk properties of materials. A typical TE cooler device is composed of many individual thermocouples. Each of these thermocouples is made of two dissimilar electrically semiconductor materials, one an n-type and the other a p-type semiconductor as form two legs connected electrically in series and thermally in parallel [7, 8]. If the electrons flowing due to an applied voltage from a material in which have average transport energy smaller than the Fermi energy (the holes in the p-type material) to another material in which their average transport energy is higher (the electrons in the n-type material), they absorb thermal energy from the lattice and this cools down the junction between the two materials. This results in a "cold side" because the electrons in the n-type material and the holes in the p-type material are carrying heat from the cold side, which means a cooling at the junctions [8, 9, 10, 11]. The most important parameter is dimensionless quantity called figure-of-merit (FOM= ZT) where T is the absolute temperature and Z is defined as: $Z \equiv S^2\sigma/\kappa$, where S is the thermoelectric power or see beck coefficient ($\Pi \equiv S \times T$), σ is the electrical conductivity can be expressed as $\sigma = |q|\mu_q n_q$ (q is the carrier charge, μ_q is carrier mobility and n_q is the carrier concentration), and κ is the total thermal conductivity [12, 13]. Further, κ is the sum of the electronic part κ_e and of the lattice part κ_{ph} [14]. Clearly, high ZT requires high S, high σ , and low κ for maximum conversion of electrical power to cooling [15]. A thermoelectric micro- and nano-cooler is a potential candidate for decreasing the operating temperature locally as well as absorbing the heat generated by these devices. The efficiency of a thermoelectric (TE) device is determined by the materials used in making the device. Thin-film thermoelectric devices have potentially higher efficiency than bulk ones due to quantum and classical size effects of electrons and phonons [16]. However, additional joule heating is generated at junctions because of the electric contact resistance, which could reduce the performance of the device [17-19]. When materials size approaches the de Broglie wavelength, their carriers become quantum confined and their energy bands then split into sub-bands characteristic of dimensional material.[1, 20]. The nanostructure materials can be considered as new materials, despite the fact that they are made of the same atomic structures as their parent materials. We considered the effect on FOM by using a single- or two-band thermoelectric material approximation such as Zinc Oxide (ZnO) [21- 25]. The low-dimensional systems provide desirable thermoelectric material properties to increase FOM [26]. Therefore, this system has been considered as one approach for increasing FOM as compared to the bulk values [26, 27]. The performance of such regime can be significantly improved where this regime make it possible to vary Peltier coefficient, electrical and thermal conductivities somewhat independently [26]. Thus, the improvements in the FOM of two-dimension quantum well are possible.

In the present work, an investigation of increase Peltier coefficient and improve heat exchange in the low dimension junction in the quantum well of ZnO using Boltzmann transport equation. ZnO has attracted a great deal of interest lately owing to the wide uses in many applications such as UV light emitters, transparent high

power electronics, surface acoustic wave devices, piezoelectric, transducers and solar cells [28].

Theoretical Considerations

Thermoelectric figure-of-merit

Most generic models of transport in solids for evaluation of the thermoelectric figure-of-merit are based on the solution of Boltzmann Transport Equation (BTE) [5, 12]. An efficient approximation for solving BTE can be attained by its linearization and through introduction of a relaxation time τ, the time period within which the system gains its equilibrium after removal of the external stimulus. Consequently, the components of the transport tensors of the system can be obtained through the relation [5, 28]:

$$L^{(l)} = \frac{vq^{2-l}}{2\pi}\int\left(-\frac{\partial f_o}{\partial E}\right)\tau(\mathbf{k})(E(\mathbf{k})-\xi)^l \mathrm{v}(\mathbf{k})\mathrm{v}(\mathbf{k})\,\mathrm{dk} \quad \text{... (1)}$$

Where,

q is the electrical carrier charge, $E(\mathbf{k})$ is the energy-wave vector dispersion relation, $\hbar\mathrm{v}(\mathbf{k}) \equiv \nabla_{\mathrm{k}}E(\mathrm{k})$ defines the velocity operator ($\hbar$ is the reduced Planck constant), and v is the valley degeneracy. Correspondingly, the measurable transport quantities are defined by the following expressions [28]: $\sigma \equiv L^{(0)}$ designates the electrical conductivity, $S \equiv \frac{1}{T}L^{(1)}\left[L^{(0)}\right]^{-1}$ and $\Pi \equiv L^{(1)}\left[L^{(0)}\right]^{-1}$ is the seebeck coefficient (since, $\Pi = S \times T$) and $K_e \equiv \frac{1}{T}\left[L^{(2)} - L^{(1)}\left[L^{(0)}\right]^{-1}L^{(1)}\right]$ is the electronic contribution to the thermal conductivity. Above, q is the electrical carrier charge, $E(k)$ is the energy-wave vector dispersion relation, $\hbar v(k) \equiv \nabla_k E(k)$ defines the velocity operator ($\hbar$ is the reduced Planck constant), and ν is the valley degeneracy. The equilibrium Fermi-Dirac distribution function is given by $f_0(E) \equiv [1 + exp(\varkappa - \xi^*)]^{-1}$, where $\varkappa \equiv E/k_BT$ (k_B is the Boltzmann constant) and denotes $\xi^* \equiv \xi/k_{\mathrm{B}}T$ the reduced chemical potential (relative to the edge of the conduction band) [5, 28].

Assuming that the current flows in the *x*-direction and the carrier mobility coincides with the bulk value, the electronic (vs. holes) contribution to the transport coefficients for bulk and quantum well σ (electrical conductivity), S (the Seebeck coefficient), and κ_e (the electronic thermal conductivity) are given by the following expressions [10, 11, 12].

$$\sigma^{3D} = \frac{e}{2\pi^2}\left(\frac{2k_{\mathrm{B}}T}{\hbar^2}\right)^{3/2}(m^*)^{3/2}\mu\, F_{1/2} \quad \text{... (2)}$$

where $m^* = \left(m_x^* m_y^* m_z^*\right)^{1/3}$ is the density of state effective mass for electrons [13], e is the electron charge, $\mathrm{k_B}$ is the Boltzmann's constant, $\hbar$ is the Plank constant divided by 2π, μ is the carrier mobility ($\equiv \langle\tau\rangle e/m^*$ hear on assuming relaxation-time approximation $\langle\tau\rangle$ is the constant) and F_{i} is the Fermi–Dirac integral defined as [13,14]

$$F_i \equiv F_i(\xi^*) = \int_0^\infty f_0 \aleph^i d\aleph \quad \text{... (3)}$$

$$n_{e,h} = \frac{1}{2\pi^2}\left(\frac{2\mathrm{k_B}T}{\hbar^2}\right)^{3/2}\left(m_{e,h}^*\right)^{3/2}\left(F_{1/2}\right) \quad \text{... (4)}$$

$$S^{3D} = -\frac{k_{\mathrm{B}}}{e}\left(5F_{3/2}/3F_{1/2} - \xi^*\right) \quad \text{...(5)}$$

$$\kappa_e^{3D}=\frac{\langle\tau\rangle {k_B}^2\,T}{3\pi^2}\left(\frac{2k_BT}{\hbar^2}\right)^{3/2}\left(m_y m_z/m_x\right)^{1/2}\left(7F_{5/2}/2-25F_{3/2}^2/6F_{1/2}\right) \quad \ldots(6)$$

In low-dimensional structures, these expressions must be reformulated. Thermo-electricity in 2-D quantum well

$$\sigma^{2D}=\frac{\langle\tau\rangle e^2}{2\pi w}\left(\frac{2k_BT}{\hbar^2}\right)\left(m_y^*/m_x^*\right)^{1/2}F_o \quad \ldots(7)$$

$$S^{2D}=-\frac{k_B}{e}\left(2F_1/F_o-\xi_{2D}^*\right) \quad \ldots(8)$$

$$\kappa_e^{2D}=\frac{\langle\tau\rangle k_B\hbar^2}{2\pi w}\left(\frac{2k_BT}{\hbar^2}\right)^2\left(m_y^*/m_x^*\right)^{1/2}\left(3F_2-4F_1^2/F_o\right) \quad \ldots(9)$$

Where

w is the width of the quantum well (layer thickness). Noticeably, $\kappa_e \gg \kappa_{ph}$ the phonon confinement to move in two-dimension may be neglected therefore can be considered κ_{ph} is constant and do not differ significantly from the bulk [5, 16, 17]. This approach can be useful to determine effects of the low dimensions on the other transport properties. More details for the thermoelectric parameters for confined electrons in low dimensions structures are given in Refs. [11, 14, 20-23].

Cooling at the Junction

Now, the relevant parameters through analytic means for ideal short base homo-junction p-n diodes; in comparison with conventional Peltier coolers, we then optimize cooling with respect to region width, current density and doping for ZnO material. Defining the Peltier coefficient in terms of carrier concentration, then, is exact in the Boltzmann limit and also good approximations in the Fermi-Dirac limit [4, 29]:

$$\boldsymbol{\Pi_e \approx -\frac{k_BT}{q}\left(ln\frac{N_C}{n}+\frac{5}{2}\right)} \quad \ldots(10)$$

$$\boldsymbol{\Pi_e \approx \frac{k_BT}{q}\left(ln\frac{N_V}{P}+\frac{5}{2}\right)} \quad \ldots(11)$$

where n and p are the electron and hole concentrations and $N_{C,V}$ is the effective density of states given by

$$N_{C,V}=2\left(\frac{m_{e,h}k_BT}{2\pi\hbar^2}\right)^{\frac{3}{2}} \quad \ldots(12)$$

The injected minority carriers are assumed to recombine at the ohmic contacts at the boundaries. The injected carrier concentration gradient is assumed to vary linearly between the edge of the depletion region and the ohmic contact, and the Peltier coefficient for injected electrons in the p-type region between the contact and the edge of the depletion region $w_p < x < -x_p$ is given by applying Equation 10 with a spatially-varying concentration:

$$\boldsymbol{\Pi_{p,e}(x)=\frac{k_BT}{q}\left\{ln\left[\frac{n_{po}}{N_C(W_p-x_p)}\times\left((x+W_p)e^{\frac{qV_j}{k_BT}}-(x+x_p)\right)-\frac{5}{2}\right]\right\}} \quad \ldots(13)$$

where V_j is the junction voltage. The $\boldsymbol{\Pi_{p,e} = \Pi_{n,e} - (V_{bi} - V_j)}$, therefore the equation 13 can be write as

$$\boldsymbol{\Pi_{p,e} = -\frac{k_B T}{q}\left(ln\frac{N_C J_o}{n_{po}(J_o + J)} + \frac{5}{2}\right)} \quad \ldots.(14)$$

Where

V_{bi} is the built-in voltage given by $V_{bi} \approx k_B T/q \, ln(N_a N_d/n_i^2)$ and J_o is the diode saturation current density given in terms of the electron and hole mobilities $\mu_{e,h}$ by $J_o = n_i^2 k_B T(\mu_e^a/W_p N_a + \mu_h^d/W_n N_d)$ where μ_e^a is the electron mobility in a region of doping concentration N_a, μ_e^a is the hole mobility in a region of doping concentration N_d, $W_p$is the p-type region width, and $W_n$is the n-type region width, J is the diode current density is related to the applied voltage by $J = J_o(exp\, qV_j/k_B T - 1)$. The heat exchange at the junction is given by

$$\boldsymbol{Q_j = J_e(\Pi_{p,e} - \Pi_{n,e}) - J_h(\Pi_{n,h} - \Pi_{p,h})}$$
$$\boldsymbol{\approx -J(V_{bi} - V_j)} \quad \ldots. (15)$$

Results and discussion

The reduced chemical potential versus carrier concentration is illustrated in figure 1. The two- and three-dimension (Bulk) reduced chemical potential (ξ^*_{3D} and ξ^*_{2D}), are compared in this figure for bulk, 20 nm, 40 nm, 60 nm, 80 nm and 100 nm thicknesses of quantum wells ZnO samples. The parameters which used in this paper to zinc oxide are shown in Table (1). The curves in these shows the carrier concentration is increased with the reduced chemical potential, moves upward in energy. The quantum confinement associated with a quantum well system causing the shifting of the band edge energy, which is one of the most interesting phenomena that occur in low dimensional system. Therefore, more asymmetry of the DOS above and below the Fermi level expected.

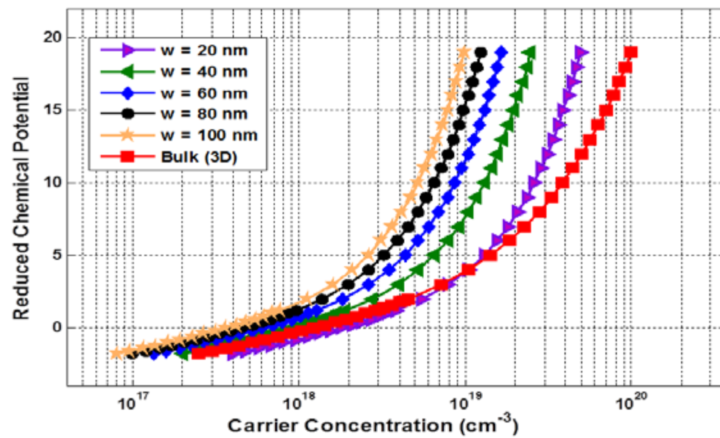

Figure (1) Carrier concentration versus reduced chemical potential (Fermi level) for 2D Quantum well and Bulk for ZnO.

From equations (5) and (8) and relationship between seebeck and peltier coefficients we found the highest value of peltier coefficient which is reached at small (w=20 nm) about (0.09 W/m-k) at the carrier concentration 10^{18}cm^{-3} as shown in figure 2. When w is increased, peltier coefficient decreases, due to lowering of density of states.

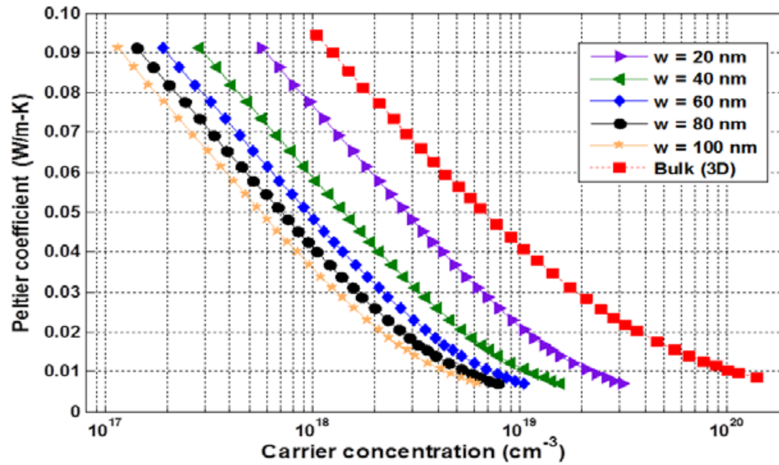

Figure (2) Peltier coefficient as a function of carrier concentration for ZnO bulk and well material.

The quantum well negatively impacts the electronic thermal conductivity of the material as a reduction can also be seen in figure 3. That means, the impact of the quantum well is to increase the peltier coefficient with only a slight increase in electronic thermal conductivity resulting in an improved power factor which is increased by a factor of (6) as shown in figure 4. This behavior is in a very good agreement with the experimentally measured power factor [30].

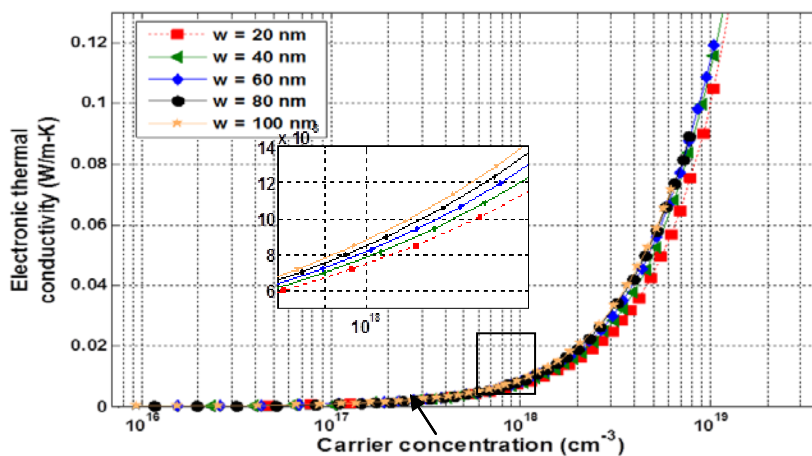

Figure (3) Electrical conductivity as a function of carrier concentration for different thickness of quantum well ZnO.

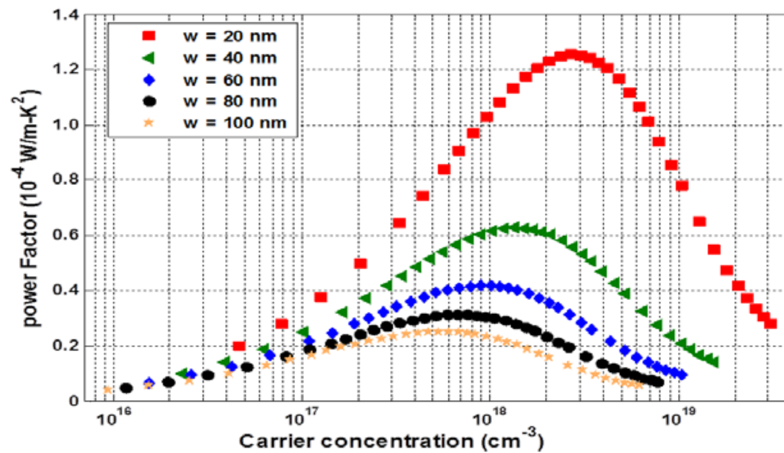

Figure (4) Calculation of power factor as a function of carrier concentration for different thickness of quantum well ZnO.

According to equations (4) and (7), there are two parameters effecting on σ, the electron mobility and carrier concentration. The present model uses the assumption of the carrier mobility unchanged as its bulk value because no interface electrons scattering. This is a conservative assumption because the scattering processes generally have an impact to decrease of carrier mobility (later we'll use different values for the electron mobility with carrier concentrations). In this case the behavior of electrical conductivity determined by the decrease of carrier concentration which results from a decrease of the sample dimension. That means, the main reason for the slight decrease in electrical conductivity of two-dimension compared with electrical conductivity of three-dimension is due to the decrease of carriers concentration. The maximum value of power factor at a given doping level coincide with the optimum reduce chemical potential (or Fermi level). This point is the optimum value between the square of the seebeck coefficient and the electrical conductivity. So it will be FOM higher the low sample dimensions and then the possibility of heat exchange and cooling thermoelectric higher and this is evident in Figure 5

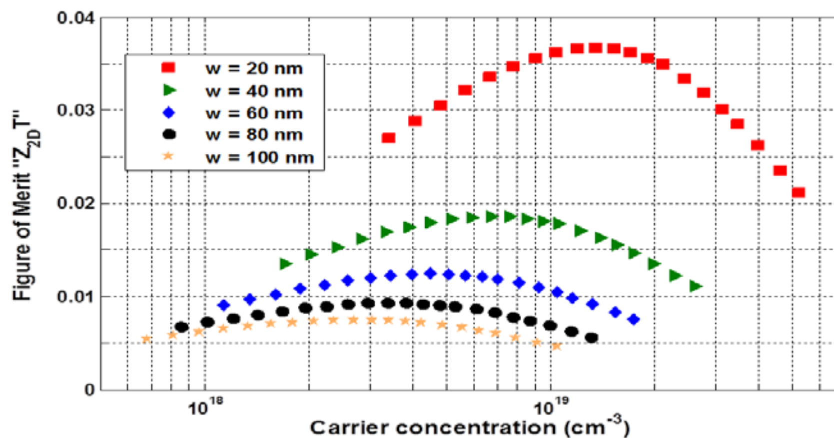

Figure (5) Figure of merit as a function of carrier concentration for different thickness of quantum well ZnO.

In the case of the ZnO diode, the amount of cooling at the junction, Q_j, and bias current density, J , were calculated as a function of the forward bias, V_j in a symmetrically doped 10 nm at two different doping levels $10^{16}cm^{-3}$ and $10^{18}cm^{-3}$, by using the equation (15) as shown in figure 6. Also the values of Q_j and J as a function of V_j for 10 nm ZnO diode. It appears that, the amount of cooling at the junctions increases with increasing the forward bias, until $V_j \approx V_{bi}$, for $V_j > V_{bi}$ joule heating predominant where the calculated values of V_{bi} for the two doping levels ($10^{16}cm^{-3}$ and $10^{18}cm^{-3}$) are (1.19V and 1.43V) respectively for ZnO doping is increased beyond the level approximated by the Boltzmann limit, i.e. $E_{fe} > E_C$ for the degenerate limit. The curves in this figure also a show that the maximum values of Q_j is 17.64 W/cm^2 for $10^{16}cm^{-3}$ doping and is 6×10^3 W/cm^2 for $10^{18}cm^{-3}$ doping. It clear that is the maximum value of Qj for lower doping occurs at lower value of V_j than that for upper doping.

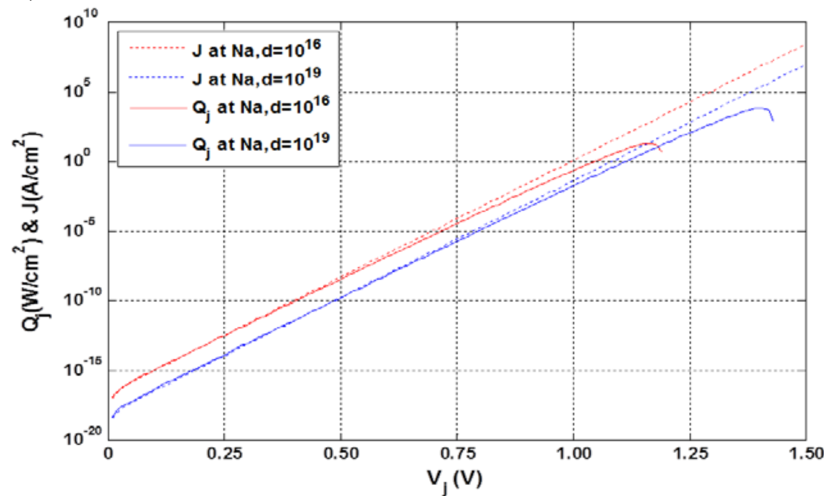

Figure (6) J and $-Q_j$ as a function of V_j in a symmetrically-doped 20 nm ZnO.

Table (1) the list of prameters that used in this paper for ZnO:

parameters	value
Electron effective mass m⊥ (a)	0.24mo
Electron effective mass m_{II} (a)	0.28mo
Hole effective mass (a)	0.59mo (⊥ = II)
Electron mobility (T = 300 K) (a)]	200cm^2/V.s
Intrinsic carrier concentration (a)	< 10^6 cm^{-3}
Electron mobility at 10^{-16} cm^{-3} (b)	90 cm^2/V.s
Electron mobility at 10^{-18} cm^{-3} (b)	260 cm^2/V.s
Hole mobility at 10^{-16} cm^{-3} (b)	0.1 cm^2/V.s
Hole mobility at 10^{-18} cm^{-3} (b)	50 cm^2/V.s
Thermal conductivity (c)	0.60 W/cm K

a, b, and c are refers to references [31], [32], [33] respectively

Conclusion

In conclusion, we have analyzed the effects of different parameters on the thermoelectric FOM using theoretical models based on employing Boltzmann transport equation for bulk and quantum well structure of ZnO. The model takes mainly into account modification of the PF due to electron confinement and evaluated the thermoelectric figure of merit. Our calculation indicates that at room temperature and above, unless there is some way to decrease thermal conductivity and increase electrical conductivity dramatically, figure of merit will not be large enough for application. The computational results show, the impact of the quantum well is to increase the peltier coefficient with only a slight increase in electronic thermal conductivity resulting in an improved power factor which is increased by a factor of (6). Verified carrier transport for internal heat exchange can facilitate the optimization of thermoelectric properties. The FOM of ZnO by doping becomes best, with an additional benefit of using the same type for legs of thermoelectric device. Therefore can be use doped ZnO diode thermoelectric whose performance is strongly dependent on the junction temperature cooling with low dimensional structures. It is found that the maximum value of the amount of cooling at the junction Qj for lower doping occurs at lower value of V_j than that for upper doping.

References

[1] Y.G. Gurevich1, and G. N. Logvinov, "Physics of thermoelectric cooling",Semicond. Sci. Technol. 20, R57–R64 (2005).

[2] A. Shakouri, J. Christofferson and Z. Bian, "High Spatial Resolution Thermal Imaging of Multiple Section Semiconductor Lasers" IEEE Photonic Devices and System Packaging Symposium, 15-16 (2002).

[3] Y. ezzahri, S. Grauby, S. Dilhaire, J. M. Rampnoux, W. Claeys, Y. Zhang, and A. Shakouri, "Determination of Thermophysical Properties of Si/Si/Ge Superlattices with a Pump-Probe Technique" Therminics, (2005).

[4] K. P. Pipe, R. J. Ram, and A. Shakouri, "Bias-dependent Peltier coefficient in bipolar devices", in International Mechanical Engineering Congress and Exposition, New York, Nov. (2001).

[5] G. Chen, and A. Shakouri, "Heat transfer in nanostructures for solid-state energy conversion", Transactions of the ASME, Vol. 124, PP.242-252 (2002).

[6] F. Meng, L. Chen and F. Sun, "Effects of heat reservoir temperatures on the performance of thermoelectric heat pump driven by thermoelectric generator" International Journal of Low-Carbon Technologies, 5, 273–282 (2010)

[7] C. Jeong, G. Klimeck, M. S. Lundstrom, "Computational Study of the Electronic Performance of Cross-Plane Superlattice Peltier Devices", Birck and NCN Publications. P. 897 (2011).

[8] S. W. Han, MD. A. Hasan , J. Y. Kim , H. W. Lee , K. H. Lee , and O. J. Kim "Multi-physics for the design and development of micro-thermoelectric coolers" . KINTEX, Gyeonggi-Do, ICCAS, Korea, PP. 1-6 (2005).

[9] Y. Zhang, M. K. Ram, E. K. Stefanakos, and D. Y. Goswami, "Synthesis, Characterization, and Applications of ZnO Nanowires", J. Nanomaterials, (2012).

[10] C. Liu, Y. Li, Y. Zeng, "Progress in Antimonide Based III-V Compound Semiconductors and Devices", Engineering, 2, Pp. 617-624 (2010).

[11] G. Chen, B. Yang, W. Liu, and T. Zeng. "Nanoscale heat transfer for energy conversion applications". Proc. Energy Conversion and Applications, Wuhan, China, Ed. Liu, Vol. 1, PP. 28-296 (2001).

[12] E. Hourdakis and A. G. Nassiopoulou, "A Thermoelectric Generator Using Porous Si Thermal Isolation" Sensors (Basel), 13(10), pp. 13596–13608 (2013).

[13]S. Farhangfar, "Size-Dependent Thermoelectricity in Nanowires", Journal of Physics D: Applied Physics 44, 12, 125403 (2011)

[14] G. Chen, A. Narayanaswamy, and C. Dames "Engineering nanoscale phonon and photon transport for direct energy conversion". Superlattices and Microstructures, Vol. 35, PP. 161-172 (2004).

[15] M. R. Jubayr, E. M-T. Salman, A. S. Kiteb, "A Theoretical Investigation of Enhanced Thermoelectric Figure of Merit of Low-Dimensional Structures", Ibn Al- Haitham j. for pure & appl. Sci., Vol.23, No. 3(2010).

[16] G. Chen , B. Yang , W. L. Liu , T. Borca-Tasciuc , D. Song , D. Achimov , M. S. Dresselhaus ,J. L. Liu , and K. Wang "Thermoelectric property characterization of Low-dimensional structures" . Presented at ICT, Beijing, China (2001).

[17] Z. H. Lan, C. H. Liang, C. W. Hsu, C. T. Wu, H. M. Lin, S. Dhara, K. H. Chen, L. C. Chen and C. C. Chen, "Nanohomojunction (GN) and Nanoheterojunction (InN) nanorods on One-Dimensional GaN Nanowire Substrates", Adv. Furct. Mater. 14, No. 3, (2004)

[18] Gelbstein,Y.; Dado, B.; Ben-Yehuda,O.; Sadia, Y.; Dashevsky, Z.; and Dariel, M.P.; High "Thermoelectric Figure of Merit and Nanostructuring in Bulk p-type $Ge_x(Sn_yPb_{1-y})_{1-x}Te$ Alloys Following a Spinodal Decomposition Reaction", Chem. Mater., Vol. 22, No. 3, PP.1054-58 (2010).

[19] I. W. Cox, and A. Tavkhelidze "Power chips for efficient energy conversion". Space Technology and Applications International, Forum-STAIF, edited by M.S.Ei-Genk, PP. 1238-46 (2004).

[20] Z. L. Wang and W. Wu, "Nanotechnology-Enabled Energy Harvesting for Self-Powered Micro-/Nanosystems", Angew. Chem. Int. Ed., 51, Pp. 2–24 (2012).

[21] A. A. Ziabari, S. M. Rozati, "Carrier transport and bandgap shift in n-type degenerate ZnO thin films: The effect of band edge nonparabolicity", Physica, B 407, Pp. 4512–4517 (2012).

[22] F. Nofeli, M. H. Tayarani, H. Arabshahi, "Electron Transport Properties in Bulk ZnO and Zn1-xMgxO Materials", Vol. 4, Issue 3, PP: 22-25 (2014)

[23. J. W. Li, L. W. Yang, Z. F. Zhou, X. J. Liu, G. F. Xie, Y. Pan, and C. Q. Sun, "Mechanically Stiffened and Thermally Softened Raman Modes of ZnO Crystal", J. Phys. Chem. B, 114, pp. 1648–1651(2010).

[24] Q. Peng, C. Liang, W. Ji, S. De, "A first principles investigation of the mechanical properties of g-ZnO: The graphene-like hexagonal zinc oxide monolayer", Computational Materials Science, 68, pp. 320–324 (2013).

[25] A. J. Leenheer, J. D. Perkins, M. F. Hest, J. J. Berry, R. P. O'Hayre, and D. S. Ginley, "General mobility and carrier concentration relationship in transparent amorphous indium zinc oxide films", Physical Review B 77, p. 115215 (2008).

[26] M. S. Dresselhaus "Nanostructures and energy conversion", In Proceedings of Rohsenow Symposium on Future Trends of Heat Transfer, (2003).

[27] Z. X. Huang, Z. A. Tang, J. Yu, S. Bai, "Thermal conductivity of nanoscale poly-crystalline ZnO thin films", Physica, B 406, Pp. 818–823 (2011).

[28] S. Farhangfar, "Thermoelectricity in Nanowires: A Generic Model", cond-mat.mes-hall, Vol.1, pp. 1–15 (2010).

[29] K. P. Pipe and R. J. Ram, "Bias-dependent Peltier coefficient and internal cooling in bipolar devices", Phys.Rev.,B 66, 125316 , (2002).

[30] D. L. Medlin, and A. Burns, "Experiment and theory are providing new insights in nanostructured thermoelectric alloys", SAND, P. 1131 (2009).

[31] Z. Fan and J. G. Lu, "Zinc Oxide Nanostructures: Synthesis and Properties",J. Nanosci. Nanotechnol., 5(10),1561-73 (2005).

[32] A. Janotti and C. G Van de Walle "Fundamentals of zinc oxide as a semiconductor", Rep. Prog. Phys. 72, p. 126501 (2009).

[33] R. D. Vispute, V. Talyansky, S. Choopun, R. P. Sharma, and T. Venkatesan, "Heteroepitaxy of ZnO on GaN and its implications for fabrication of hybrid optoelectronic devices", Appl. Phy. lett. Vol. 73, No. 3 (1998)